NASA TM- 79266

NASA-TM-79266 19790023172

A Reproduced Copy

OF

NASA TM- 79266

Reproduced for NASA

by the

NASA Scientific and Technical Information Facility


NF00525

LIBRARY COPY

JUL 16 1984

LANGLEY RES. . .
LIBRARY, NAS
HAMPTON, VIRGINIA

FFNo 672 Aug 65

79N31342*# ISSUE 22 PAGE 2924 CATEGORY 20 RPT#: NASA-TM-79266
E-181 79/00/00 20 PAGES UNCLASSIFIED DOCUMENT

UTTL: Sputtering in mercury ion thrusters
AUTH: A/MANTENIEKS, M. A.; B/RAWLIN, V. K.

Cleveland, Ohio. AVAIL.NTIS SAP: HC A02/MF A01
Presented at 14th Intern. Conf. on Electric Propulsion, Princeton, N. J., 31 Oct. - 2 Nov 1979; sponsored by AIAA and Deutsche Gesselschaft fur Luft-und Raumfahrt

MAJS: /*GROUND TESTS/*MERCURY ION ENGINES/*SPUTTERING/*THIN FILMS
MINS: / CHEMISORPTION/ GAS PRESSURE/ ION CURRENTS/ NITROGEN
ABA: M.M.M.
ABS: A model, which assumes that chemisorption is the dominant mechanism, is applied to the sputtering rate measurements of the screen grid of a 30 cm thruster in the presence of nitrogen. The model utilizes inputs from a variety of experimental and analytical sources. The model of environmental effects on sputtering was applied to thruster conditions of low discharge voltage and a discussion of the comparison of theory and experiment is presented.

ENTER:

NASA TM-79266

SPUTTERING IN MERCURY ION THRUSTERS

Maris A. Mantenieks* and Vincent K. Rawlin*
National Aeronautics and Space Administration
Lewis Research Center
Cleveland, Ohio

Abstract

Ground based tests of Hg ion thrusters have identified sputter-erosion of thruster components as one of the main life limiting phenomena Subsequent measurements have revealed that sputtering rates can be affected by background gases at pressures as low as 10^{-7} torr. With the recent interest in thin film technology, sputtering in the presence of reactive gases has been studied in great detail. This paper presents the results of many of those studies and applies them to the sputtering of electric thrusters. A model, which assumes that chemisorption is the dominant mechanism, is applied to the sputtering rate measurements of the screen grid of a 30-cm thruster in the presence of nitrogen. The model utilizes inputs from a variety of experimental and analytical sources The model of environmental effects on sputtering was applied to thruster conditions of low discharge voltage and a discussion of the comparison of theory and experiment is presented

E-181

Introduction

Ground based life tests of mercury ion thrusters have identified sputter-erosion of thruster components as one of the main life limiting phenomena.[1,2] Subsequent measurements have shown that thruster component sputtering can be affected by background gases at pressures as low as $1x10^{-7}$ torr.[3] This effect makes the correlation of the results of ground and space tests very difficult

The reduction of sputtering rates due to background facility gases has been previously recognized [4-6] However, the magnitude and the criteria for occurrence of this effect have not been well defined In recent work, related to thin film technology, the effects of reactive gases on film deposition have been studied in detail [7-13] These deposition studies, as well as some recent sputtering studies,[14-19] have greatly increased the knowledge of the effects of reactive gases on the sputtering/deposition process

This paper will first present a review of the observed effects of background gases on sputtering Results from thruster tests and data from other sources will be presented A brief review of the details of interactions of gases with surfaces is then presented followed by a discussion of a model of basic sputtering phenomena in the presence of background gases Comparisons are then drawn between the models and the results obtained in a 30-cm mercury ion thruster

Effects of Background Gases on Sputtering

Sputtering of Thruster Components

Reference 3 describes the effect of facility residual gases on the sputtering rate of the ion optics screen grid of a mercury ion thruster as determined from direct grid thickness and molybdenum spectral intensity measurements. Figure 1 (from ref 3) shows the sputtering rates from grid measurements operated in two different facilities as a function of test facility pressure The facility pressure was dictated by the temperature of the cold wall and the gas pumping speed for the particular tests. For discharge chamber voltages between 35 to 37 volts, a large decrease of the screen grid sputtering rate is observed with increasing facility pressure. At a discharge voltage of 32 volts, the sputtering rate is considerably reduced at a given pressure due to a decrease of ion energy as well as a reduction of multiply charged ions in the thruster.

Figure 2 shows the spectral intensity of atomic molybdenum which was sputtered from the screen grid, as a function of nitrogen pressure. Nitrogen was introduced directly onto the facility beginning at the no load pressure of about $1x10^{-7}$ torr. Nitrogen was chosen for the test because of its availability and the fact that in this facility at no load conditions, it was found to be the most abundant single species of the residual gases (~25%). Data are shown for discharge voltages of 40, 45, and 50 volts. As the nitrogen pressure is increased (Fig. 2) there is a decrease in the molybdenum spectral line (MoI) intensity associated with sputtered screen grid material. Similar trends in the direct sputtering rate measurements were observed as the facility pressure was varied (Fig. 1).

As pointed out in Ref. 3, the observed molybdenum spectral intensity is expected to be proportional to the sputtering rate of the screen grid if the thruster plasma conditions are held constant. Assuming the plasma density, electron temperature, plasma spatial distributions, and charge state of the ions are negligibly affected by the background pressure, the spectral intensity in Fig 2 should be proportional to the sputtering rate for a given discharge voltage This assumption was verified in Ref. 3 as spectral intensities of neutral and ionized mercury were found to be essentially constant with nitrogen pressure up to the low 10^{-5} torr range

Figure 2 shows that the molybdenum spectral intensity increases substantially as the discharge voltage is raised from 40 to 50 volts Because the plasma conditions are dependent on the discharge voltage, the spectral intensity cannot be correlated directly to the sputtering rate for different discharge voltages It is clear, that at the 50-volt condition the MoI line intensity and thus the sputtering rate of the screen grid reaches a plateau around the $2x10^{-7}$ torr level This plateau represents the "clean metallic surface" or simulated space condition At a discharge voltage of 45 volts it is not certain if a plateau has been reached At 40 volts and below, a plateau is not reached Therefore, the sputtering rates of a 30-cm thruster operating at normal conditions of discharge voltage of 32 volts are affected by background gases because pressures less than $1x10^{-7}$ torr are not readily available for thruster tests

*Aerospace Engineers

N79-31343#

It should be pointed out that the spectral data of Ref. 3 was plotted as a function of the partial pressure of nitrogen, but may also include effects due to other gases which have been found to be reactive.[19] Therefore, it was decided to plot the total facility pressure, rather than the partial pressure of nitrogen, for all data presented herein. At the higher pressures, the effect of the other gases becomes negligible.

In order to show the effect of background gases as a function of ion energy, the screen grid was biased negatively, with respect to its normal cathode potential. Based on the results of steady state thruster electrical parameters and spectral analyses of the thruster discharge, the bias did not significantly perturb the plasma conditions. The results of the bias tests, shown in Fig. 3 (from Ref. 3), were taken at a discharge voltage of 50 volts and a beam current of 2 A. Here the spectral line intensity was normalized to the maximum intensity for each bias test. The data show that the curve is shifted slightly to the right or higher pressure with increasing ion energy.

These data will be subsequently used in the section dealing with the sputtering model.

Review of Environmental Effects on Sputtering Rates

The sputtering characteristics shown in Figs 1 to 3 are similar to those observed by others studying the effects of reactive gases. Data which evaluated the sputtering rate directly[6,13,14,16] and those that inferred sputtering rates by measuring deposition rates[7,11,12] are found in literature. Typical curves from these references are shown in Fig. 4 for various combinations of ion type, ion energies, and target material. It is observed that the magnitude of the change of the sputtering rate with pressure ranges from about a factor of 10 (similar to results observed in thrusters with a Mo-N_2 system) to no change at all for Au and Ag-O_2 systems. The latter result is similar to that obtained in the thruster tests with increasing argon and mercury background pressure.[3] It should be pointed out that deposition data usually underestimate the magnitude of the change of the sputtering rate of the metal target.

As shown in Fig. 4, the effect has been reported in the literature at pressures considerably higher than those found in Figs. 1 to 3. This is most probably due to the higher energy of the ions employed in those studies. To obtain a more exact comparison the ion current density also has to be considered. Increasing the current density shifts the curve toward higher pressure, at a given ion energy.[3,11]

Another parameter of interest is the pressure range over which the change in sputtering rate takes place. In the 30-cm thruster (Figs. 1 to 3) the sputtering rate decreased over two orders magnitude of pressure. In some tests (Fig. 4) the sputtering rate variation occurred over a very narrow pressure range, in a nearly step-like fashion. As will be discussed later, this difference may be due to the differences in the degree of reactivity between the target surface and the background gas.

Interactions of Gases with Metals

The adsorption of gas by metals is due to a field force at the surface of the solid, which attracts the gas. The forces of attraction may be physical or chemical and the terms physisorption and chemisorption are generally used to distinguish the different interactions.

Physisorption. The three kinds of forces that are responsible for physisorption are attractive dispersion forces, short range repulsive forces, and forces due to permanent dipoles within the adsorbed molecules.[20] The binding energy of these forces are weak as characterized by the heats of adsorption and are on the order of 0.1 to 0.2 eV.[26] Because of the weak bonding energies involved, physisorption is not considered to be a dominant mechanism inside the thruster,[21] where the component temperatures are about 350° C. However, because a molecule can jump from site to site many times before desorption, physisorption may play an important role in the kinetics of dissociative chemisorption as a precursor state.[22,23]

Chemisorption. Chemisorption is defined as the adsorption of atoms or molecules involving electron transfer or sharing with surface atoms. Generally, there are three types of chemisorption processes identified: molecular, dissociative, and sorption layer formation.[21] Molecular chemisorption is characterized by heats of adsorption about 0.5 eV.[21] In dissociative chemisorption, heats of adsorption may be as high as 8 eV.[26] Chemisorption is usually limited to a coverage of one monolayer or less. With some very reactive systems, such as Ta-O_2, and Mo-O_2, much more than a monolayer can be adsorbed and this is referred to as sorption layer formation.[21] Because of the relatively high temperature inside a thruster, dissociative chemisorption is believed to be the dominant mechanism. Reference 24 demonstrated chemisorption of N_2 on molybdenum at temperatures up to 900° C. Studies have shown that nitrogen chemisorption is limited to about a monolayer,[21,26,27] a fact of importance in the sputtering model to be discussed.

Chemisorption phenomena are highly specific to the surface material and the gas involved. For example, according to Refs. 21, 26, and 27, nitrogen will be chemisorbed by W, Ta, Mo, Ti, Zr, Hf, V, and Nb. Changes in the sputtering or deposition rate of Mo,[3,7,16] Ti,[7] Ta,[16] W,[16] have been found in the presence of nitrogen. There appears to be some ambiguity about a class of elements which apparently do not chemisorb nitrogen, but may form nitrides.[28] These include Al, Si, Ni, and Fe. Changes of deposition rates have been reported by Ref. 7 with Al and Fe in nitrogen atmospheres. Elements such as Ag and Au do not chemisorb nitrogen or form nitrides,[21,27] however no sputtering data exists in the literature for these systems.

Model of Sticking Coefficient for Chemisorption

The chemisorption process, in many cases, can be described by a simple model of sticking coefficient behavior as a function of coverage. If θ_{oo} represents the probability that two neighboring sites are empty, and if physisorption jumps are negligible, then the sticking coefficient, s, is given by[23]

$$s = s_o\theta_{oo} = s_o\left\{1 - \theta - \frac{2\theta(1-\theta)}{[1 - 4\theta(1-\theta)B]^{1/2} + 1}\right\} \quad (1)$$

where

$B \quad 1 - e^{\omega/kT_s}$

θ fraction of surface covered with adsorbed species

T_s surface temperature

ω pairwise interaction energy

s sticking coefficient

s_o sticking coefficient at $\theta = 0$

k Boltzmann constant

The pairwise interaction energy, ω, is negative for repulsive and positive for attractive interactions For repulsive forces B possesses two limits of zero at $\omega/T_s = 0$ and one at $\omega/T_s = -\infty$. For large attractive forces (i e., $\omega \to \infty$) B becomes $-\infty$. B may be taken as the measure of the degree of short range order in the chemisorbed layer.[23]

For purposes of the paper it is sufficient to look at only the limiting cases of Eq (1) For large repulsive interactions energies with $B = 1$ we have

$$\left.\begin{aligned} s &= s_o(1 - 2\theta) \quad \text{for } \theta \le 0.5 \\ s &= 0 \quad \text{for } \theta \ge 0.5 \end{aligned}\right\} \quad (2)$$

If there is no short range order in the chemisorbed layer and $B = 0$ then

$$s = s_o(1 - \theta)^2 \quad (3)$$

which is the expression for dissociative adsorption [23] For the large attractive nearest neighbor interaction, Eq. (1) becomes

$$s = s_o(1 - \theta) \quad (4)$$

which is usually referred to as the Langmuir isotherm

Equations (2) to (4) are plotted in Fig 5 Also shown are measured relative sticking coefficients of nitrogen on both molybdenum films[21] and (110) crystals.[29] The experimental sticking coefficient data appear to follow the $(1 - \theta)^2$ relationship more closely than the forms given in Eqs (2) or (4) Because the exact sticking coefficients are not available for partially ionized and dissociated nitrogen, the general relationship of Eq (1) cannot be used For this study Eqs. (3) and (4) will be chosen for the sticking coefficient functions, because $s_o(1 - \theta)^2$ best approximated the dissociative chemisorption data and $s_o(1 - \theta)$ probably best represents the larger expected sticking coefficient value due to the dissociated and ionized nitrogen inside the thruster

In order that more than one monolayer be allowed to be chemisorbed, Ref 7 includes an effective sticking coefficient $s_{eff} = s_o(1 - \theta)^n$ where P_o is the saturated vapor pressure, and n is related to the number of chemisorbed layers Because the Mo-N_2 system appears to form only about one monolayer this factor will not be included in this study

Sputtering Model

Several mechanisms have been suggested in the literature to account for the decrease of the sputtering rate of metals in the presence of reactive gases. One mechanism postulates that for certain metal-gas systems an insulating layer is formed at the target allowing a surface charge to build up which retards the incident ion. Thus, the energy of the ions and the observed sputtering rate would be reduced.[8] Most other studies do not consider this effect and conclude that the incident ion energy is unchanged and the actual sputter yield of the chemisorbed surface layer formed is reduced.[7,16] This is the mechanism assumed for the model described herein.

Following Hrbek,[16] it is assumed that the sputtered flux of the metal surface F_θ, is a linear combination of the sputtered fluxes at full coverage $F_{\theta=1}$ and that of a clean metal target $F_{\theta=0}$. In that case

$$F_\theta = F_{\theta=0}(1 - \theta) + F_{\theta=1}\theta \quad (5)$$

F_θ can be correlated with the sputtering data of Figs. 2 and 3, because the spectral intensity is assumed to be directly proportional to the sputtered molybdenum flux

The equilibrium chemisorption-sputtering process can be described by a simple rate equation

$$sZ(P)_{atom} = F_A \ , \ cm^{-2}\ sec^{-1} \quad (6)$$

where

s sticking coefficient

$Z(P)_{atom}$ arriving flux of reactive gas atoms

F_A removal flux of adsorbed gas atoms

The species of particles removed during the sputtering process in the presence of a reactive gas may be either in the atomic, molecular, or ionic state [30-32] Usually, the fraction of molecular and ionic species is considered to be small. Winters and Sigmund[33] concluded that only nitrogen atoms were sputtered from tungsten Therefore, in the rate equation for the removal flux, F_A, was chosen which describes atomic removal mechanism. If molecular removal were to be considered, F_A^2 would have to be used in Eq (6) [34]

The ratio of sputtering at a given level of adsorption to that of a clean metal surface was defined as $F_\theta/F_{\theta=0}$, which can be calculated by eliminating θ from Eqs (5) and (6) and choosing one of the sticking coefficient functions

Selection of $s = s_o(1 - \theta)$ results in

$$\frac{F_\theta}{F_{\theta=0}} = 1 - \frac{s_oZ(P)}{s_oZ(P) + F_A}\left(1 - \frac{F_{\theta=1}}{F_{\theta=0}}\right) \quad (7)$$

The choice of $s = s_o(1 - \theta)^2$ results in

$$\frac{F_o}{F_{\theta=0}} = \frac{(2s_o mZ(P) - F_A) + \sqrt{[F_A - 2s_o mZ(P)]^2 + 4s_o Z(P)[F_A - s_o m^2 Z(P)]}}{2s_o Z(P)} \qquad (8)$$

where

$$m = \frac{F_{\theta=1}}{F_{\theta=0}}$$

A discussion will follow concerning the assumptions in evaluating each parameter in Eqs. (7) and (8).

Adsorption Rate

Z(P) represents the total flux of reactive gas particles arriving at the target surface. That flux can be evaluated by kinetic theory, with the assumption that in equilibrium the number of reactive particles entering and leaving the thruster are equal. This implies that there is no steady state gettering of reactive gases inside the discharge chamber.

The flux of molecules of reactive gas arriving at the screen grid surface is

$$Z(P)_{mol} = \frac{3.5\times10^{22}\,P}{\sqrt{MT_w}},\ cm^{-2}\ sec^{-1} \qquad (9)$$

where

P partial pressure of reactive gas, torr

M molecular weight of the reactive gas, amu

T_w temperature of reactive gas taken to be equal to the facility wall temperature, K

The flux of atoms chemisorbed on the target surface is equal to $2s_oZ(P)_{mol}$. Because nitrogen is chemisorbed dissociatively $Z(P)_{atom}$ is used in Eq. (5). P was obtained from the total gas pressure gauge inside the vacuum facility. Because of the discharge plasma processes, the nitrogen incident on the screen grid consists of a variety of species including N_2, N_2^+, N, and N^+. It is of interest to know the fraction of each species inside the thruster because the sticking coefficients of each species may be different. Estimates, using the model of Refs. 36 and 37, indicate that only about 2 percent of the nitrogen is ionized or dissociated inside a 30-cm thruster operating at 2 A beam and a 50 volt discharge voltage. The sticking coefficient, s_o, of N^+ and N on molybdenum at the thruster experimental conditions have been measured to be between 0.75 and 1.0.[36]

Values found in the literature of the sticking coefficient, s_o, for molecular nitrogen on clean molybdenum vary from 0.02 to 0.9.[21,24,29,37] One of the reasons for the large variation in values of the sticking coefficient is that the studies have included many different kinds of surfaces such as filaments, thin films, and single crystals. All of the calculations made herein assume only dissociative nitrogen chemisorption and a value of 0.75 was chosen as a representative sticking coefficient on clean molybdenum for this study.[21,37] The other values of parameters used for the evaluation of Eqs. (7) and (8) were T_w = 100 K and M = 28.

In this study, it is assumed that no mercury is adsorbed on the molybdenum surface. The data available gives inconclusive results. Refs. 39 and 40 show zero coverage above 275° to 325° C. On the other hand, Ref. 41 indicates two desorption peaks at 100° to 230° C and 440° to 520° C. This implies that some mercury coverage is still possible at the steady state screen grid temperature of 350° C.

Total Removal Rate

The removal rate, F_A, could include evaporation and sputtering. Desorption spectra of chemisorbed nitrogen on molybdenum indicate that evaporation commences at about 500° C.[24,29,41] Reference 9 finds that Mo_2N films formed by sputtering molybdenum in the presence of nitrogen are stable at 400° C and 8×10^{-6} torr. Because the screen grid temperature of a thruster is less than that temperature, it was assumed that sputtering is the only significant removal mechanism of the adsorbed gas. Therefore, the sputtered flux, F_A, may be written as,

$$F_A = \frac{J_{Hg}T}{e}\left[S_G{}^{+}\frac{J_{Hg}{}^{++}}{2J_{Hg}T}\,(S_G{}^{++} - 2S_G{}^{+})\right] \qquad (10)$$

where

$J_{Hg}T$ total mercury ion current density, A/cm^2

$J_{Hg}{}^{++}$ doubly ionized current density, A/cm^2

$S_G{}^{+}$ sputter yield of adsorbed gas by singly charged ions

$S_G{}^{++}$ sputter yield of adsorbed gas by doubly charged ions

e elementary charge per ion

It is usually assumed that $(S_G{}^{++})_E = (S_G{}^{+})_{2E}$, where E is the ion energy. The average value of $J_{Hg}T$ was determined to be 3.4×10^{-3} A/cm^2 from the measured saturated ion current to the screen grid at a beam current of 2 A.

The current density profile of a 30-cm thruster is not uniform. It is likely that the optical spectrometer measurements indicated molybdenum intensities representative of average values rather than peak values. Therefore, an average current density $J_{Hg}T$ was chosen for the calculation. A value of 0.109 for the ratio $J_{Hg}{}^{++}/2)_{Hg}T$ was obtained when the data of Ref. 42 was extrapolated to a discharge voltage of 50 volts.

It is believed that the parameter S_G contains the greatest uncertainty in the calculations. There has been very little experimental work done in measuring the sputter yields of adsorbed gases. Reference 33 measured yields of nitrogen chemisorbed on tungsten by various inert gas ions. Reference 43 has measured sputtering cross sections (sputter yield x number of atoms in a monolayer coverage) of sulfur chemisorbed on nickel as sputtered by inert gas ions. Sputtering data is compared to theoretical models and agreement is claimed by both authors. Best agreement between theory and data appears in Ref. 33 for the heavy inert gases such as xenon and krypton. The values of S_G used for this study were calculated using the theory of Ref. 33. The model and calculations are presented in the appendix. The three possible collision mechanisms con-

sidered, as shown in Fig. 6, are: (I) direct knock-off by the collision of the incident ion and adsorbed atom, (II) removal of adsorbed atom due to reflected incident ions, and (III) sputtering of adsorbed atom due to collision of adsorbed atom with the sputtered target atom. It is found that at low ion energies, direct knock-off by incident ions of adsorbed atoms (mechanism I) represents from half to all of the total sputter yield (Ref. 33 and appendix). Mechanism II contributions are uncertain due to the uncertainty in the value of the reflection coefficient, R_{12}, to be used for Mo-N_2 systems. Two values of R_{12} were chosen to bound the values of the sputter yield calculated for mechanism II. Values of sputter yield, calculated for mechanism III, were found to be negligible for the ion energies of interest herein. Values of sputter yields calculated for each mechanism are presented in the appendix.

Values of S_G^+ and S_G^{++} were chosen from the curves of the sputter yield of adsorbed nitrogen (Fig. A-1) as a function of ion energy for each value of R_{12} used. An ion energy of 50 eV was selected to correspond to the thruster discharge voltage of 50 volts. The removal fluxes, corresponding to these sputter yields, calculated from Eq. (10) are 5.22×10^{15} atoms/cm^2 sec (for R_{12} = 0.5) and 2.29×10^{15} atoms/cm^2 sec (for R_{12} = 0). Winters and Sigmund state that the lower value of R_{12} is probably more realistic.

Magnitude of the Effect

The ratio of the molybdenum sputtering rates of the completely covered surface, $F_{\theta=1}$, and the clean surface, $F_{\theta=0}$, was obtained from the low and high pressure plateaus of Fig. 3 for a discharge voltage of 50 volts and zero bias. A value of 0.1 was obtained. Figure 1 also indicates that a value of about 0.1 is appropriate for a discharge voltage of 36 volts. At this time there is no known model which may be used to predict the magnitude of the reduction of the sputtering rate in the presence of a reactive gas at low ion energies. Reference 44 suggests that the magnitude be evaluated from the ratio of binding energies of the clean metal surface and the compound formed with the reactive gas. This is proposed because according to Sigmund's[45] sputtering theory at intermediate ion energy ran[illegible] the sputter yield is inversely proportional to the binding energy of a substance. The results, however, are not conclusive and actual data (Fig. 3) was used for the calculation.

Comparison of Experiment with Sputtering Model

Figure 7 shows the comparison of the experimental data of the zero bias curve of Fig. 3 with the sputtering model (Eq. (7)). The two curves using $F_A = 5.22\ 10^{15}$ and 2.29×10^{15} atoms/cm^2 sec represent the two limiting values used for the sputtering yield of the adsorbed gas. It is evident that the choice of the lower value of S_G, which assumed an ion reflection coefficient of zero, is in good agreement with the experimental data. This result indicates that the direct collision (mechanism I) is probably the dominant sputtering process. It should be noted that the ratio of limiting values $F_{\theta=1}/F_{\theta=0}$ in Eq. (7) was obtained from the experimental data of Fig. 3.

The removal rate, F_A, can also be calculated from Eqs. (4) and (6) with $\theta = 1/2$ as

$$F_A = s_o Z(P_{\theta=1/2}) \qquad (11)$$

from which an effective sputtering yield $S_{G,eff}$ can be obtained from the following equation,

$$s_o Z(P_{\theta=1/2}) = \frac{J_{Hg}T}{e} S_{G,eff} \qquad (12)$$

with $Z(P_{\theta=1/2})$ evaluated at $P_{\theta=1/2}$ where

$$\frac{F_{\theta=1/2}}{F_{\theta=0}} = \frac{1}{2}\frac{F_{\theta=1}}{F_{\theta=0}} + 1$$

$S_{G,eff}$ represents a sputter yield where the different charged ion species are averaged. Equation (11) results in a removal rate of 2.67×10^{15} atoms/cm^2 sec. Use of Eq. (12) gives a value of $S_{G,eff}$ equal to 0.126 atoms/ion. Table 1 presents the values of $S_{G,eff}$ calculated for the other curves of Fig. 3. Comparison of these values with those presented in Table A-1 for S_G (with $R_{12} = 0$) indicate that S_G^+ is in good agreement with $S_{G,eff}$ at a given ion energy. This occurs because the ratio of $J_{Hg}^{++}/2J_{Hg}T$ from Eq. (10) is small and S_G does not increase rapidly with ion energy.

As previously discussed, various models of the sticking coefficient can be used. The two functions chosen were $s = s_o(1 - \theta)$ and $s = s_o(1 - \theta)^2$. Figure 8 shows the comparison of the two sticking coefficient models using $F_A = 2.67\times10^{15}$ atoms/cm^2 sec. It was noted before that for dissociative nitrogen adsorption the $s = s_o(1 - \theta)^2$ equation approximated some data found in literature. In Fig. 8 it appears that to fit the experimental data of this study $s = s_o(1 - \theta)$ is a better approximation. This may be due to the small but very reactive fraction of nitrogen atoms and ions present in the thruster discharge chamber.

Discussion of Criteria for Predicting the Onset of Environmental Effects

Several criteria have been developed in the past for evaluating conditions for clean surface sputtering. A brief discussion will follow on each of these.

Flux ratio. Yonts and Harrison[46] derived one of the earliest criteria in 1960. It requires that the ion beam density incident on the target should be much greater than the particle density of the background gases. At 1×10^{-6} torr, where an effect in the thruster is observed, the ratio for our experimental conditions becomes

$$\frac{J_{Hg}T}{Z(P_{10^{-6}\ \mathrm{torr}})} = \frac{2.12\times10^{16}}{5.1\times10^{14}}\ \frac{\text{ions}}{\text{mol}} \gg 1$$

Therefore, the mercury ion flux to the screen grid is found to be much greater than the molecular nitrogen flux. Thus, the criteria is found to be inadequate for the conditions of our study.

Poisoning ratio. The ability of the ions to sputter the adsorbed gas is the important criterion. Therefore, a "poisoning ratio" was defined in Ref. 47 as the ratio of the arrival flux of reactive gas to the removal flux of the target atoms (including the adsorbed gas). This ratio was used for Al-O_2 systems bombarded with high energy (2.5 to 10 keV)

ions where the sputter yields of the adsorbed gas and clean metal are probably comparable. As shown earlier, the large differences in sputter yields between the adsorbed gas (nitrogen) and the clean metal (molybdenum) at low ion energies lead to a modified "poisoning ratio," equivalent to Eq. (6), which requires the use of the sputter yield of the adsorbed gas

Transition pressure. Reference 11 defines a transition pressure, P_o (torr), at which a chemical reaction takes place between the target surface and the chemisorbed gas

$$P_o = \frac{3\times10^{-5}\ R}{\Delta G} \qquad (13)$$

where

R sputtering rate of the clean target, Å/min

P_o partial pressure of reactive gas, torr

ΔG Gibbs' free energy function for the reaction, kcal/mole

The author claims excellent agreement between his model and sputtering and thin film deposition measurements, but it will be shown, that this equation in its present form appears not to be valid at the ion energy range of our interest

As shown in Figs 2 and 3, the pressure range over which the effect takes place is quite large (~2 orders of magnitude), therefore, the definition of P_o is difficult to define P_o may be determined approximately from the data of Fig. 3 as the point where the tangent at the center of the curve (point of symmetry) deviates from the curve at the lower part of the curve The transition pressure values of the four data curves from Fig. 3 are listed in Table 1 These values of P_o, as a function of bias, are compared to the behavior of P_o as predicted in Eq (13) and are shown in Fig 9. The calculated transition pressures were obtained by using the appropriate sputter yields of molybdenum from Ref 48 In order to compare the relative behavior of Eq. (13) with the results from the data of Fig. 3, the curve was normalized to a point where the discharge voltage was 50 volts and zero grid bias.

It is apparent that the calculated P_o, based on the metallic sputter yield predicts a much larger increase with ion energy than was obtained from Fig. 3. A much better agreement is found when the transition pressure is assumed to be proportional to the sputter yield of the adsorbed gas The sputter yields, $S_{G,eff}$, were obtained by using Eq (12) and the data of Fig 3 and are listed in Table 1 Equation (12) shows that for = 1/2 the shift with pressure of the sputtering rate curves is proportional to the sputter yield of the gas $S_{G,eff}$.

The agreement claimed by Castellano may occur because at high ion energies where his studies were made, the sputter yields of the adsorbed gas and the target clean surface may be about equal [3] At low ion energies, as found in our study, the sputter yields of the adsorbed gas and the target metal appear to be quite different Our limited amount of data suggests that the sputter yield of the gas rather than the target should be used in calculating the transition pressure, P_o, from Eq (13)

Estimated Environmental Effect at Discharge Voltage of 32 V

Normal operating conditions of a 30-cm diameter Hg ion thruster are a beam current equal to 2 A and a discharge voltage equal to 32 volts. At these conditions, as pointed out earlier, the sputtering rate is affected by the facility environment. The model that has been developed in this study offers a means of calculating the effect at a given facility pressure. Data in this study has been presented dealing only with nitrogen, therefore the extrapolation to discharge voltage of 32 volts can only strictly apply to nitrogen pressure in the facility According to Ref. 19 all residual gases tested that are found in a typical vacuum facility showed sputtering characteristics similar to that of nitrogen. However, in order that the effect of all residual gases be included in the model more sputtering data will be required along with a better understanding of how various gases are adsorbed and sputtered on a surface in the presence of each other It should also be recalled that many assumptions were made in the model where accurate information was lacking in the literature such as the sticking coefficient function, the neglect of mercury adsorption on the target surface, neglect of other possible removal mechanisms, and finally the many assumptions that went into the calculation of the sputter yield of the adsorbed gas.

The estimated environmental effect of nitrogen, at a discharge voltage of 32 volts, is seen in Fig. 10. This curve is a plot of Eq. (7), using the sputter yield of nitrogen at 32 volts as obtained from the appendix $F_{\alpha=1}/F_{\alpha=0}$ was chosen to be the same as for discharge voltage of 50 volts. From Fig. A-1, it is evident that at this low voltage, the curve for the sputter yield is much steeper than at the higher ion energies. Therefore, a small error in the ion energy will result in a rather large change in the calculated sputter yield which will lead to a correspondin error in Fig. 10

The temperature of the screen grid is cooler at the normal operating conditions than those for the conditions of Fig. 3. This may result in an increase of mercury adsorption on the screen grid surface, thus complicating the adsorption-sputtering processes discussed in this study Neglecting these possibilities, it is seen from Fig 10 that operation of a thruster in nitrogen atmosphere at 1×10^{-7} torr, results in a sputtering rate of the molybdenum screen grid which is only about 12 percent less than that of clean surface conditions

Conclusions

In the past, sputtering rates of ion thruster components have been observed to decrease substantially as the background gas pressure in the test facility was increased Relative sputtering rates of the screen grid have been determined by spectral intensities as functions of various thruster parameters in the presence of one of the reactive gases, such as nitrogen, generally found in a vacuum facility In this paper surface-gas interactions are discussed that are thought to be possible for the environmental effect Chemisorption was found to be the mechanism that most likely leads to a reduction of the sputter yield of a surface in the presence of a reactive gas. A model was presented

which appeared to be in general agreement with the experimental results. It assumes that sputtering is the only removal mechanism of the chemisorbed gas. The sputtering yield of the adsorbed gas is shown to be a determining factor of the sputtering rate of a metal target in the presence of a reactive gas. A sputtering yield of the adsorbed gas was calculated using the theoretical model of Winters and Sigmund It was found that at the low ion energies existing in an ion thruster, sputter yields of adsorbed gases are substantially higher than the sputter yields of metals considered.

It was found that models are available which show promise in determining the onset of an environmental effect. However, determining the magnitude of the effect, at least at low ion energies, one must still rely upon experimental methods.

An attempt was made to predict the magnitude of the environmental effect at normal operating thruster conditions of 32 volts and 2 A beam. At these conditions it is impossible to measure the effect experimentally due to large vacuum facility limitations. It is concluded that the effect is not large at 1×10^{-7} torr of nitrogen pressure However, it is felt that more data is required in order that models presented in this study can be applied to general thruster test facility conditions.

Appendix - Theoretical Model of Sputter Yields of Chemisorbed Gases

The model of Winters and Sigmund[33] assumes the sputtering process of chemisorbed gases on a metal surface to be due to a series of binary elastic collisions involving the bombarding ions, the metal target and the adsorbed gas. With similar arguments, Sigmund has been able to calculate, with reasonable accuracy, the sputter yields of "clean" materials at intermediate and high energies [45]

The sputtering process is postulated to be composed of three mechanisms,[33] as illustrated in Fig. 6, which include

(I) An incident ion collides directly with an adsorbed nitrogen atom, which is then reflected from the target lattice The scattering process is approximated by Thomas-Fermi power cross section with a Born-Mayer zero power interaction chosen for low energy ions. The contribution to the sputter yield of atomic nitrogen due to this mechanism is obtained by combining Eqs (8) and (5) of Ref 33 (assuming a zero power interaction) to yield

$$S_I = \frac{n_3 C_{13}}{\cos\theta} (\ln x) \qquad (A1)$$

where

$$x = \frac{\gamma_{13} E}{U_3}, \quad \gamma_{ij} = \frac{4M_iM_j}{(M_i + M_j)^2}, \quad C_{13} - C_o = \frac{1}{2}\pi\lambda_o a^2$$

n_3 number of atoms contained in a saturated monolayer

a screening radius equal to 0 219 Å[45]

A_o constant equal to 24[45]

E incident ion energy, eV

U_3 binding energy of the adsorbed atom, eV

M molecular weight

θ angle of incidence of the ion

C_o constant

(Particle subscripts are defined in Fig. 6.) Sigmund states that the screening radius or the constant λ_o may be off as much as a factor of 2.[45]

(II) The incident ion penetrates into the target and is eventually reflected. On its way out it knocks off an adsorbed atom. The ratio of this sputtering yield, S_{II}, to that of S_I is derived to be:[33]

$$\frac{S_{II}}{S_I} = R_{12}\left[4 - \frac{4 \log x}{3(x^{1/3} - 1)}\right]\cos\theta \qquad (A2)$$

where R_{12} is an experimentally measured ion reflection coefficient dependent on the angle of incidence and ion energy. This calculation assumes a power interaction of $m = 1/3$, but according to Winters and Sigmund it is sufficiently accurate for a qualitative estimate to be compared to $m = 0$ interactions.

(III) The incident ion sputters a target atom, when the ion is ejected it knocks off an adsorbed ion. The contribution from this process is calculated by:

$$S_{III} = 4\gamma_{23}C_{23}\frac{U_2 n_3 S_{12}}{U_3}\frac{(1 - [(1 + \log y)/y])}{(1 - \gamma_{23}/y)^2} \qquad (A3)$$

where

$y = \gamma_{12}\gamma_{23}F/U_3$

$C_{23} \cong C_o$

U_2 ≈ sublimation energy of the target

S_{12} sputtering rate of clean target at ion energy E

Assuming that the sputtering processes are additive, the total sputtering yield becomes

$$S_G = S_I + S_{II} + S_{III} \qquad (A4)$$

Discussion of Model

Table A-1 shows the calculated sputtering yields for each of the three mechanisms described above for nitrogen chemisorbed on molybdenum and bombarded by mercury ions. In making these calculations several assumptions were made, which will now be discussed.

The constant, n_3, in Eq. (A1) was taken to be 1×10^{15} atoms/cm^2 This number represents a monolayer coverage in which approximately each surface target atom has one chemisorbed nitrogen atom attached to it Under normal molecular dissociative adsorption conditions, less than a complete monolayer of nitrogen on molybdenum is possible Under conditions, such as existing on a mercury thruster the presence of molecular or atomic nitrogen, adsorption sites may be filled which normally are not [28]

Difficulty arises in choosing the proper value of the binding energy, U_3, because of the lack of available data in the literature. Winters and Sigmund approximate the binding energy for atoms as one-half the sum of the dissociation energy and the heat of adsorption. For a W-N_2 system they estimated this value to be 6.7 eV For lack of a

better number, the same value will be used here for Mo-N_2 system.

The ion reflection coefficient, R_{12}, represents a parameter which is also not readily available in the literature. There even appears to be some ambiguity in defining the reflection coefficient.[30] For most gas ions incident on a clean tungsten surface the reflection coefficient of 10^{-4} to 10^{-2} have been measured for ion energies between 100 to 1000 volts [30] Values between 0.1 and 0.4 (increasing with decreasing ion energy) have been measured for alkaline metal ions on a molybdenum surface.[30] It has been observed that R_{12} appears to increase with increasing impurity levels on a target surface Winters and Sigmund believe that S_{III} was overestimated by their choice of R_{12} equal to 0.6 Therefore, following their example, two values of S_G are presented in Table 1, one which assumes R_{12} equal to 0.5 and the other equal to zero.

It is evident from Table A-1 that contributions to S_G from S_I and S_{II} (when $R_{12} = 0.5$) dominate. Only at energies much larger than 100 volts does S_{III} contribute significantly to the total sputtering yield S_G.[33]

Figure A-1 summarizes the various sputter yields of nitrogen on molybdenum as a function of mercury ion energy. Shown are the two calculated curves of S_G using the two limiting values of the reflection coefficient. For comparison the sputtering yields of nitrogen chemisorbed on tungsten, as sputtered by xenon ions,[33] as well as the sputtering yield of "clean" molybdenum by Hg ions are also shown. As pointed out in the main text of this report, best agreement between theory and thruster experiments was found when the S_G values with $R_{12} = 0$ was used. Similar results were found by Winters and Sigmund. Steep decrease in S_G for ion energies less than 40 eV remains to be verified experimentally.

References

1. Collett, C , "Thruster Endurance Test," Hughes Research Labs., Malibu, Calif., May 1976 (NASA CR-135011).

2 Collett, C. R and Bechtel, R T , "An Endurance Test of a 900 Series 30-cm Engineering Model Ion Thruster," AIAA Paper 76-1020, Nov 1976

3. Rawlin, V. K. and Mantenieks, M A , "Effect of Facility Background Gases on Internal Erosion of the 30-cm Hg Ion Thruster," AIAA Paper 78-663, Apr. 1978.

4. Yonts, O. C , Normand, C E , and Harrison, D E , Jr , "High-Energy Sputtering," Journal of Applied Physics, Vol 31, Mar 1960, pp 447-450

5 Almen, O and Bruce, G , "Collection and Sputtering Experiments with Noble Gas Ions," Nuclear Instruments and Methods, Vol 11, 1961, pp 257-278

6. Hasseltine, E. H., Hurlbut, F. C., Olson, N. T., and Smith, H P., Jr., "Cesium-Ion Bombardment of Aluminum Oxide in a Controlled Oxygen Environment," Journal of Applied Physics, Vol. 38, Oct. 1967, pp. 4313-4316.

7. Abe, T. and Yamashira, T., "The Deposition Rate of Metallic Thin Films in the Reactive Sputtering Process," Thin Solid Films, Vol. 30, 1975, pp. 19-27.

8. Hollands, E. and Campbell, D. S., "The Mechanisms of Reactive Sputtering," Journal of Materials Science, Vol 3, 1968, pp. 544-552.

9. Nagata, S and Shoji, F., "Structure of Film Prepared by Low Energy Sputtering of Molybdenum," Japanese Journal of Applied Physics, Vol. 10, Jan. 1971, pp. 11-17.

10. Gerstenberg, D. and Calbick, C. J., "Effects of Nitrogen, Methane, and Oxygen on Structure and Electrical Properties of Thin Tantalum Films," Journal of Applied Physics, Vol. 35, Feb. 1964, pp. 402-407.

11. Castellano, R. N , "Reactive Ion Beam Sputtering of Thin Films of Lead, Zirconium, and Titanium," Thin Solid Films, Vol. 46, 1977, pp. 213-221.

12. Castellano, R. N., "Reactive Sputter Etching of Thin Films for Pattern Delineation," IEEE Transactions on Components, Hybrids, and Manufacturing Technology, Vol. CHMT-1, Dec. 1978, pp. 397-399.

13. Bomchil, G., Buiguez, F , Monfret, A., and Galzin, S , "Reactive Sputtering of Indium Targets in D C Triode Configuration," Thin Solid Films, Vol. 47, 1977, pp. 235-240.

14. Cantagrel, M. and Marchal, M., "Argon Ion Etching in a Reactive Gas," Journal of Materials Science, Vol 8, 1973, pp. 1711-1716.

15. Heller, J., "Reactive Sputtering of Metals in Oxidizing Atmospheres," Thin Solid Films, Vol 17, 1973, pp 163-176

16. Hrbek, J , "Sputtering of Metals in the Presence of Reactive Gases," Thin Solid Films, Vol 42, 1977, pp 185-191.

17. Shinoki, F and Itoh, A., "Mechanism of RF Reactive Sputtering," Journal of Applied Physics, Vol 46, Aug. 1975, pp 3381-3384.

18. Stirling, A J and Westwood, W D., "A Spectroscopic Investigation of the Reactive Sputtering of Aluminum," Thin Solid Films, Vol. 7, 1971, pp 1-10.

19 Beatie, J R , "A Model for Predicting the Wearout Lifetime of a 30-cm Mercury Ion Thruster," AIAA Paper 79-2079, Oct 1979

20. Gregg, S J. and Sing, K. S W., Adsorption, Surface Area, and Porosity, Academic Press, New York, 1967

21. Fromm, E. and Mayer, O., "Interaction of Oxygen and Nitrogen with Clean Transition Metal Surfaces," Surface Science, Vol. 74, 1978, pp. 259-275.

22. Ehrenreich, H., ed., Solid State Physics - Advances in Research and Applications, Vol. 30, Academic Press, New York, 1975, p. 139.

23. King, D. A. and Wells, M. G., "Reaction Mechanism in Chemisorption Kinetics: Nitrogen on the {100} Plane of Tungsten," Proceedings of the Royal Society of London, Series A, Vol. 339, Aug. 1974, pp. 245-269.

24. Oguri, T., "Chemisorption of Nitrogen on Molybdenum," Journal of the Physical Society of Japan, Vol. 19, Jan. 1964, pp. 77-83.

25. Ignatiev, A. and Jona, F., "The Structure of Overlayers. III. Nitrogen on Mo {001}," Surface Science, Vol. 49, 1975, pp. 189-200.

26. Morrison, S. R., The Chemical Physics of Surfaces, Plenum Press, New York, 1977, p. 197.

27. Winters, H. F. and Kay, E., "Influence of Surface Adsorption Characteristics on Reactively Sputtered Films Grown in the Biased and Unbiased Modes," Journal of Applied Physics, Vol. 43, Mar. 1972, pp. 794-799.

28. Winters, H. F. and Horne, D., "The Chemisorption of Nitrogen at Activated Sites on a Polycrystalline Tungsten Surface," Surface Science, Vol. 24, 1971, pp. 587-611.

29. Mahnig, M and Schmidt, L. D., "Adsorption of H_2 and of N_2 on {110} Mo," Zeitschrift für Physikalische Chemie (Frankfurt am Main), Vol. 80, 1972, pp. 71-81.

30. Carter, G. and Colligon, J. S., Ion Bombardment of Solids, American Elsevier Pub. Co , New York, 1968.

31. Benninghoven, A. and Müller, A , "Investigation of Surface Reactions by the Static Method of Secondary Ion Mass Spectrometry," Surface Science, Vol. 39, 1973, pp 416-426.

32. Hofer, W. O. and Martin, P J., "On the Influence of Reactive Gases on Sputtering and Secondary Ion Emission," Applied Physics, Vol. 16, 1978, pp. 271-278

33. Winters, H F and Sigmund, P , "Sputtering of Chemisorbed Gas (Nitrogen on Tungsten) by Low Energy Ions," Journal of Applied Physics, Vol. 45, Nov 1974, pp 4760-4766.

34. Dushman, S , Scientific Foundations of Vacuum Technique, Wiley, New York, 1949, p. 410.

35. Wilbur, P J , "Mercury Ion Thruster Research, 1978," Annual Report, Dec 1977-Dec. 1978, Colorado State University, Fort Collins, Colo , Dec. 1978 (NASA CR-159485)

36. Wilbur, P. J., "A Model for Chemisorption in Ion Thrusters," AIAA Paper 2062, To be Presented at the 14th International Electric Propulsion Conference, Princeton, N.J., Oct. 30-Nov. 1, 1979.

37. King, D. A. and Tompkins, F. C., "Sticking Probabilities, Redistribution Phenomena and Desorption Spectra for Nitrogen on Molybdenum and Titanium Films," Transactions of the Faraday Society, Vol. 64, 1968, pp. 496-506.

38. Winters, H. F., "Ionic Adsorption and Dissociation Cross Section for Nitrogen," Journal of Chemical Physics, Vol. 44, Feb. 1966, pp. 1472-1476.

39. Bennette, C. J., "Behaviour of Various Adsorbates on Metal Substrates," Field Emission Corp., McMinnville, Oreg., Feb. 1966. (NASA CR-54704)

40. Swanson, L. W., Strayer, R. W., and Davis, L. E., "Desorption, Mobility and Work Function Change of Mercury on Tungsten and Molybdenum Substrates," Surface Science, Vol. 9, 1968, pp. 165-186.

41. Reynolds, T. W., Unpublished data.

42. Vahrenkamp, R. P., "Measurement of Doubly Charged Ions in the Beam of a 30-cm Mercury Bombardment Thruster," AIAA Paper 73-1057, Oct. 1973.

43. Taglauer, E , Beitat, U., Marin, G., and Heiland, W., "Sputtering of Adsorbed Layers by Ion Bombardment," Journal of Nuclear Materials, Vol. 63, 1976, pp 193-198.

44. Kelly, R. and Lam, N , "The Sputtering of Oxides, Part 1 A Summary of Experimental Results," Ion Surface Interaction, Sputtering and Related Phenomena, edited by R. Behrisch, Gordon and Breach Science Publishers, New York, 1973, pp. 37-45.

45. Sigmun , P , "Theory of Sputtering I - Sputtering Yields of Amourphous and Polycrystalline Targets," Physical Review, Vol. 184, Aug. 1969, pp. 383-416.

46. Yonts, O. C and Harrison, D. E., Jr , "Surface Cleaning by Cathode Sputtering. Journal of Applied Physics, Vol. 31, Sep. 1960, pp. 1583-1584

47. Andrews, A E., Hasseltine, E. H., Olson, N T , and Smith, H. P , Jr., "Cesium Ion Sputtering of Aluminum," Journal of Applied Physics, Vol. 37, 1966, pp. 3344-3347.

48. Askerov, Sh G and Sena, L. A , "Cathode Sputtering of Metals by Slow Mercury Ions," Soviet Physics - Solid State, Vol. 11, Dec. 1969, pp. 1288-1293.

TABLE 1. - EFFECTIVE SPUTTERING YIELD OF ADSORBED NITROGEN AS CALCULATED FROM EQ. (12) AND TRANSITION PRESSURE AS OBTAINED FROM FIG. 3

Ion energy (discharge voltage + bias), V	$S_{G,eff}$, atoms/ion	Transition pressure, P_o, torr
50	1.26×10^{-1}	7×10^{-6}
60	1.73×10^{-1}	8×10^{-6}
70	2.10×10^{-1}	9×10^{-6}
80	2.34×10^{-1}	1×10^{-5}

TABLE A1. - CONTRIBUTIONS OF VARIOUS SPUTTERING MECHANISMS OF CHEMISORBED NITROGEN ON MOLYBDENUM BOMBARDED WITH MERCURY IONS

[$n_3 = 1\times10^{15}$, $U_3 = 6.7$ eV, $C_o = 1.8\times10^{-16}$.]

Ion energy, eV	S_I	S_{II}		S_{III}	$S_G = S_I + S_{II} + S_{III}$	
		$R_{12} = 0$	$R_{12} = 0.5$		$R_{12} = 0$	$R_{12} = 0.5$
30	1.6^{-2}	0	1.83^{-2}	2.04^{-5}	1.6^{-2}	3.43^{-2}
40	6.78^{-2}	0	8.03^{-2}	6.55^{-5}	6.78^{-2}	1.48^{-1}
60	1.41^{-1}	0	1.75^{-1}	4.11^{-4}	1.41^{-1}	3.16^{-1}
80	1.93^{-1}	0	2.46^{-1}	1.31^{-3}	1.94^{-1}	4.40^{-1}
100	2.33^{-1}	0	3.04^{-1}	2.99^{-3}	2.36^{-1}	5.39^{-1}

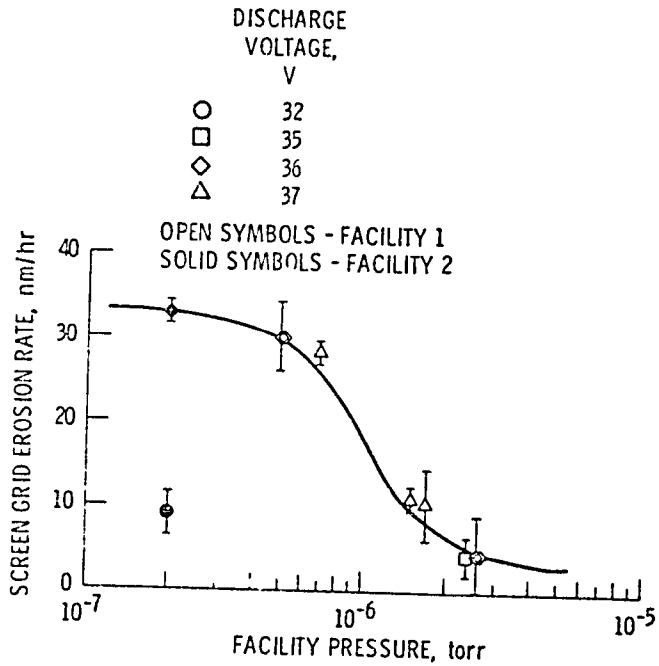

Figure 1. - Screen grid erosion rate as a function of facility pressure Beam current, 2 A (fig. 14 of ref. 3).

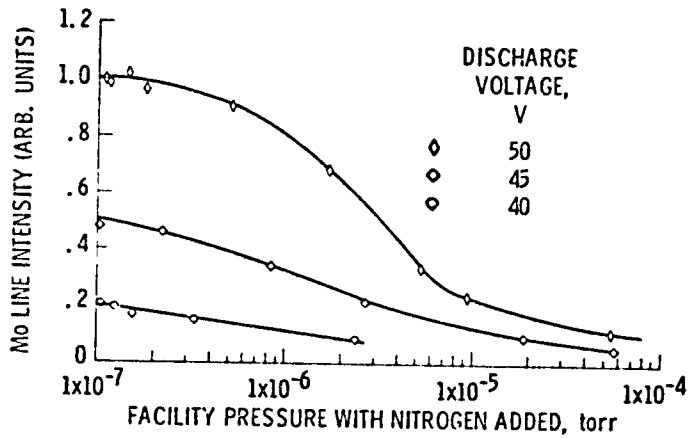

Figure 2. - MoI (3798.8 nm) line intensity as a function of facility pressure with nitrogen added. Beam current, 2 A.

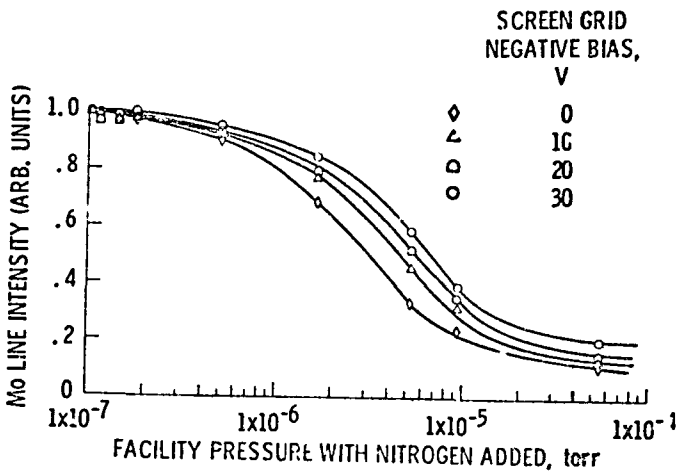

Figure 3. - MoI (3798.8 nm) line intensity as a function of facility pressure with nitrogen added. Beam current, 2 A, discharge voltage, 50 V.

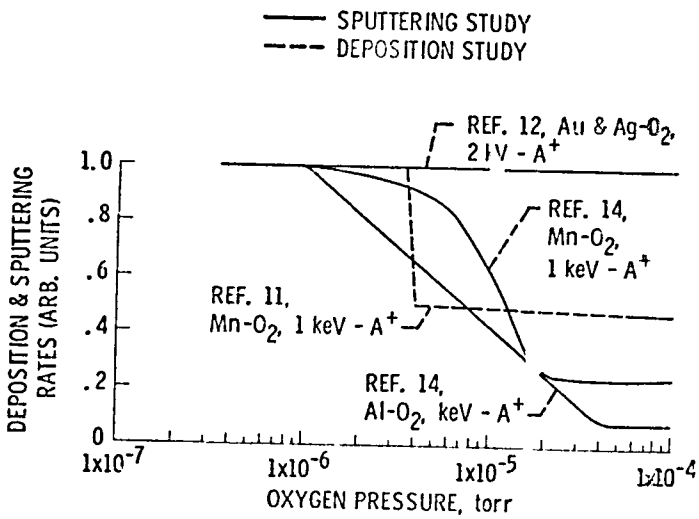

Figure 4. - Comparison of various sputtering and deposition rates in the presence of oxygen.

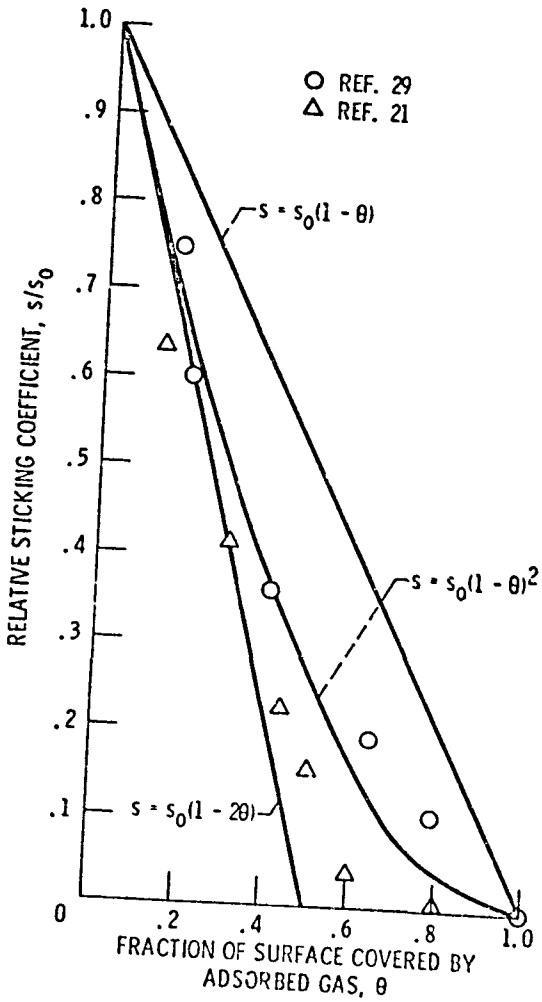

Figure 5 - Comparison of sticking coefficient functions

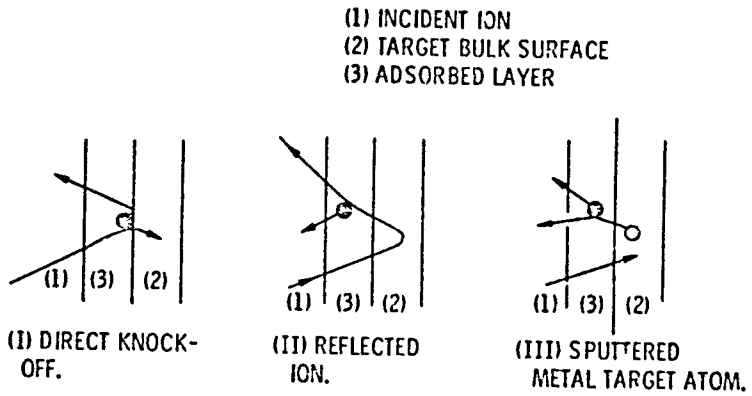

Figure 6. - Postulated sputtering mechanisms of adsorbed gas (ref. 33).

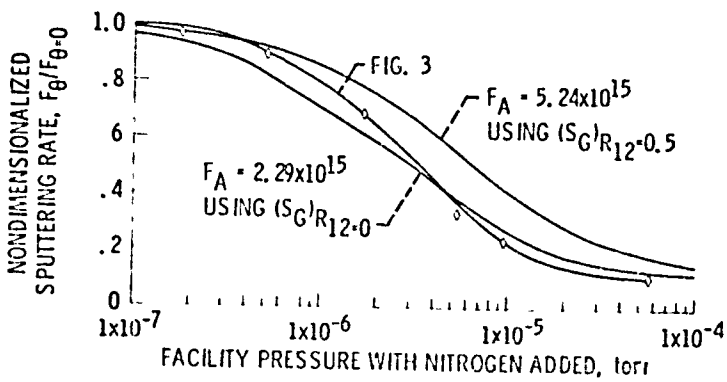

Figure 7 - Comparison between sputtering data and model (eq (7)) for limiting values of s_G, as a function of facility pressure

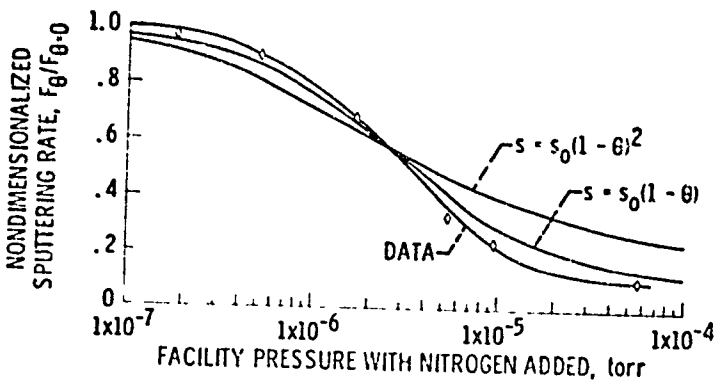

Figure 8. - Comparison between sputtering data (fig. 3) and eqs. (7) and (8) as a function of facility pressure with nitrogen added. Discharge voltage, 50 V, 0 bias, beam current, 2 A.

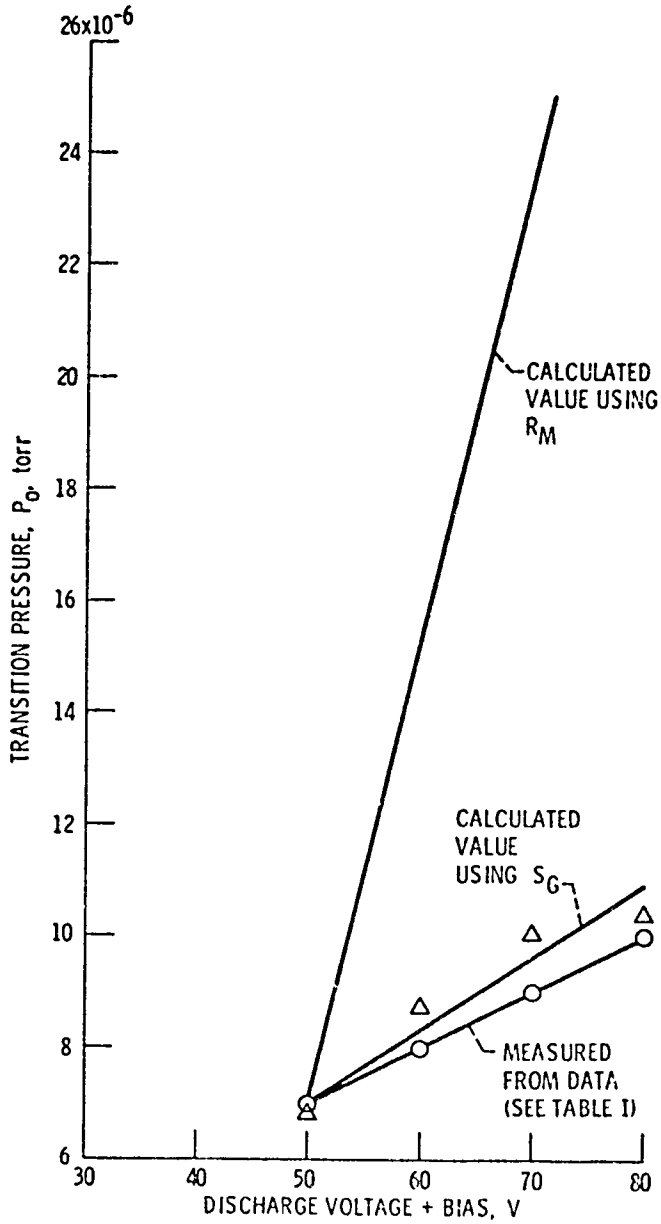

Figure 9 - Comparison between measured and calculated (eq (13)) transition pressure as a function of effective ion energy.

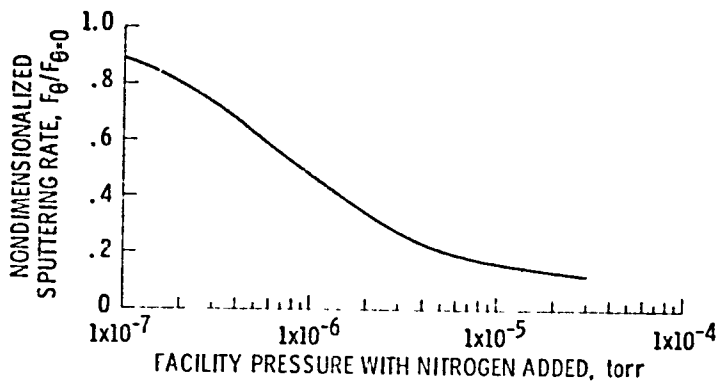

Figure 10. - Estimated sputtering rate (eq (7)) as a function of facility pressure with nitrogen added at a voltage of 32 V and beam current of 2 A.

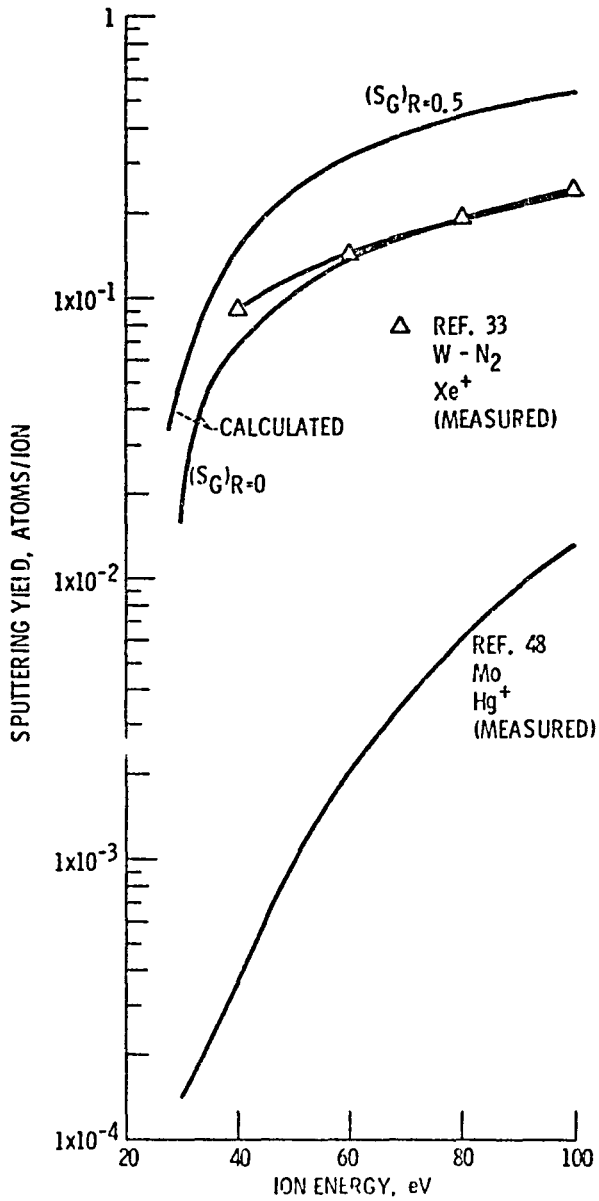

Figure A-1 - Comparison of calculated and measured sputtering yields as a function of ion energy

END

DATE

FILMED

NOV 9 1979

End of Document